



Deposited via The University of Leeds.

White Rose Research Online URL for this paper:

<https://eprints.whiterose.ac.uk/id/eprint/103147/>

Version: Accepted Version

Article:

Al-Tahmazi, T and Babatunde, AO (2016) Mechanistic study of P retention by dewatered waterworks sludges. *Environmental Technology & Innovation*, 6. pp. 38-48. ISSN: 2352-1864

<https://doi.org/10.1016/j.eti.2016.05.002>

© 2016, Elsevier. Licensed under the Creative Commons Attribution-NonCommercial-NoDerivatives 4.0 International <http://creativecommons.org/licenses/by-nc-nd/4.0/>

Reuse

Items deposited in White Rose Research Online are protected by copyright, with all rights reserved unless indicated otherwise. They may be downloaded and/or printed for private study, or other acts as permitted by national copyright laws. The publisher or other rights holders may allow further reproduction and re-use of the full text version. This is indicated by the licence information on the White Rose Research Online record for the item.

Takedown

If you consider content in White Rose Research Online to be in breach of UK law, please notify us by emailing eprints@whiterose.ac.uk including the URL of the record and the reason for the withdrawal request.

Mechanistic study of P retention by dewatered waterworks sludges

T. Al-Tahmazi^{a,b} and A.O. Babatunde^{a,*}

^aHydro-environmental Research Centre, Energy and Environment Theme,
Cardiff University School of Engineering, Queen's Buildings, The Parade,
CF24 3AA, Cardiff, Wales, UK.

^bCollege of Engineering, University of Karbala, Karbala, Iraq

*Corresponding author: babatundea@cardiff.ac.uk

Abstract

Eutrophication caused by excess phosphorus (P) loading poses serious environmental risk to freshwater bodies around the world. Advancing our fundamental understanding towards practical reduction of this risk using novel industrial by-products as P adsorbents is the focus of this study. The study examined the combined effect of solution chemistry and the inherent properties of a novel adsorbent (dewatered waterworks sludges) on their P retention. The overall aim was to contribute to a mechanistic understanding of P retention by the sludges; and to better understand what properties regulate their P retention. Results confirm a strong but variable affinity for P by the sludges. Aluminium (Al)-based sludges generally had higher total specific surface areas; and tended to have higher P sorption capacities (6.09 - 26.95 mg-P/g) than iron (Fe) - based sludges (5.83 -23.75 mg-P/g). In most cases, adsorption data was well fitted with the Freundlich model. However, data for two of the Al-based sludges was best described by the Langmuir model with very minimal leaching of Al, Calcium (Ca) and sulphate (SO_4^{2-}) ions observed; indicating surface complexation via P binding into the Al hydr(oxide) as the main mechanism for these Al-based sludges.

Principal component and multiple linear regression analyses revealed that the metal content (Al, Fe, $\text{Al}_{\text{oxalate}}$ and $\text{Fe}_{\text{oxalate}}$) and total specific surface area components had the most significant explanation for the variance of: (i) P-uptake at different initial P concentrations; (ii) the adsorption maxima; and (iii) the Freundlich constant (K_f); ($p < 0.001$). Total carbon (TC),

29 organic carbon, Ca content and exchangeable Ca components explained a significant
30 reasonable variance in P-uptake and K_f . This explanation was demonstrated for the role of Ca
31 content in chemical P precipitation mechanism; and also for exchanging TC sites on the
32 surface of the sludges with phosphate ions via ligand exchange mechanism. Overall, giving
33 the combined effect of intrinsic sludge properties and solution chemistry; dewatered
34 waterworks sludges with high reactive metal content (Al and Fe), Ca and SO_4^{2-} ions, and total
35 specific surface area would be the best choice for P retention in practical applications.

36

37 Keywords: adsorption capacity, aluminium sludges, dewatered waterworks sludges, ferric
38 sludges, phosphorus

39

40 **1. Introduction**

41 Eutrophication caused by excess phosphorus (P) loading poses serious environmental risk to
42 freshwater bodies around the world. It has now become a global environmental concern
43 particularly with waters worldwide experiencing major increases in P concentrations leading to
44 additional drinking water treatment, decreased biodiversity and loss of recreational value. For
45 example, P fluxes to oceans have increased approximately 2.8-fold since the industrial
46 revolution and over 400 coastal dead zones can be found at the mouths of rivers discharging
47 P (Diaz and Rosenberg, 2008). Surveys in the United States and the European Union (EU)
48 estimates that 78% and 65% of their coastal areas, respectively, exhibit symptoms of
49 eutrophication (Mayer et al., 2013); whilst inland waters are equally at risk. According to the
50 U.S. Environmental Protection Agency, eutrophication is the biggest overall source of
51 impairment of the nation's rivers and streams, lakes and reservoirs, and estuaries; while in the
52 EU, approximately 50% of all lakes have total P (TP) at levels which pose a risk of
53 eutrophication (Bogestrand, 2004). In the UK, the Technical Advisory Group has advised that
54 65% of England's rivers fail current P limits with lakes being more sensitive to contamination
55 (Wood et al., 2007).

56 In order to prevent eutrophication of inland and coastal waters, legislation on P discharge into
57 the surrounding environment is becoming stricter worldwide and many water companies now
58 face additional treatment requirements to reduce P in their final effluent discharges.
59 Consequently, water companies are now faced with the prospect of having to implement
60 additional treatment methods in order to supplement their traditional biological, chemical and
61 physical processes for reducing P. However, finding the best application to reduce P can be
62 challenging, particularly when low consents are required, coupled with the expectation to strive
63 towards recovering the P.

64

65 In this regards, P removal via adsorption on novel materials and by-products is gaining
66 increased attention as an environmentally friendly and cost-effective means of removing and
67 reducing P in wastewater streams, and enabling its recovery. This study focuses on one of
68 such novel by-products, dewatered waterworks sludges which is a widely available by-product
69 of drinking water purification processes; and which have been shown to be effective adsorbent
70 for P (Babatunde et al., 2009). However, while the sludges can retain P and therefore be used
71 as an adsorbent for P removal; there is a need to further investigate the factors that influence
72 their P retention behaviour. This is because drinking water treatment plants use different water
73 sources and different coagulants and polyelectrolytes; and therefore, they produce sludges
74 with variable elemental compositions and characteristics. Whilst some studies have examined
75 the influence of either solution chemistry or physicochemical characteristics of the sludges on
76 their P retention; investigation into their combined effects over a wide range of samples from
77 various sources has been limited. This is, however, crucial for improving our mechanistic
78 understanding of their P retention behaviour and for their effective practical use for P removal.
79 Therefore, the specific objectives of this study were: (i) to evaluate the physicochemical
80 properties of seventeen dewatered waterworks sludges from different sources; and together
81 with the solution chemistry effects, relate these to their P retention behaviour; (ii) to probe the

82 characteristics of P retention by the dewatered waterworks sludges; and (iii) to investigate and
83 determine the mechanisms involved in P retention by the sludges.

84

85 **2. Material and Methods**

86 **2.1 General Physicochemical characterization**

87 Dewatered waterworks sludges were collected from seventeen drinking water treatment works
88 located in the United Kingdom. The treatment plant locations are kept anonymous on request;
89 and samples obtained were simply labelled using a sequential alphabetic code generated from
90 the location names. To determine the chemical composition, 0.1g samples of each of the
91 sludges (air dried and ground to particle size <2mm) was digested with 3 mL of HCl and 3 mL
92 of HNO₃ in a microwave and analysed using inductively coupled plasma atomic emission
93 spectroscopy (ICP-AES). Chloride, sulphate and exchangeable calcium ions were determined
94 by extraction with deionized water at a 1:10 solid:liquid ratio for 4 hours, followed by filtration
95 with 0.45 µm membrane filters. The chloride and sulphate ions were measured using Ion
96 Chromatography (ICS – 2000 Ion Chromatography system) while Ca concentration was
97 measured using ICP-AES. Total carbon (TC) and OC were determined by Total Organic
98 Carbon Analyzer (TOC-V CSH (Shimadzu)); pH was determined following the British
99 Standards institution method (British Standards Institution, 1990). The total surface area was
100 measured with the sludges in a wet condition using Ethylene Glycol Monoethyl Ether (EGME)
101 method. The method determines both the internal and external surface areas where adsorption
102 and ion exchange take place (see Cerato and Lutenegger (2002) for the measuring
103 procedure). The morphological structure of the sludges was examined by X-ray diffraction
104 (XRD); the scattering angles ranged from 2° to 80° 2θ with scanning speed at 0.02° 2θ per 0.5
105 second. To quantify the amorphous Al and Fe oxides of the sludges, ammonium oxalate-
106 extractable Al and Fe were measured according to the method described by McKeague and
107 Day (1966).

108 **2.2 Adsorption isotherm study**

109 P sorption maxima of the dewatered water sludges was determined by equilibrating 1g each
110 of the dewatered sludges samples in 200 ml acid-washed polyethylene bottles. The bottles
111 contain 100 ml solution at three pH values (4, 7 and 9); and seven initial P concentrations (5,
112 10, 20, 40, 80, 160 and 320 mg-P/l). Hydrochloric acid (0.01M) and potassium hydroxide
113 (0.1M) were used for pH adjustment. Potassium dihydrogen phosphate (KH_2PO_4) was used to
114 prepare P stock solution. After 48-hours pre-determined equilibration time, samples were
115 filtered using a 0.45 μm membrane filter and analysed for P using a HACH DR-3900
116 spectrophotometer. The mass of P adsorbed per mass of adsorbent (q) in mg/g was calculated
117 using Eq. (1).

$$118 \quad q_e = \frac{(C_o - C_e)}{m} V \quad (1)$$

119 where C_o and C_e are the initial and equilibrium P concentrations, respectively in the solution
120 (mg/l), V represents the volume of the solution (l), and m is the mass of the adsorbent (g).

121 The equilibrium data was fitted with Langmuir and Freundlich isotherm models; the linearized
122 forms of which are given below, respectively in equations 2 and 3;

$$123 \quad \frac{C_e}{q_e} = \frac{1}{bQ_o} + \frac{C_e}{Q_o} \quad (2)$$

$$124 \quad \log q_e = \log K_f + \frac{1}{n} \log C_e \quad (3)$$

125 where b is constant of Langmuir adsorption (L/g), Q is the maximum mass of P adsorbed at
126 saturation conditions per mass unit of adsorbent (mg/g); K_f is the bonding energy related
127 constant (L/g), and n is Freundlich heterogeneity constant.

128 **2.3 P retention – Mechanism and linkage with inherent properties**

129 **2.3.1 Exchangeable ions and Precipitation tests**

130 In order to investigate the possible mechanism of P retention by the sludges through calcium
131 phosphate precipitation and/or adsorption to the precipitated aluminium and iron oxides,
132 exchangeable ions and precipitation tests were carried out. For the exchangeable ions test,
133 the leachability of Ca, Al and Fe from the sludges was determined by shaking 1 g each of the
134 sludge samples in 100 ml of deionized water at three initial pH solutions (4, 7 and 9), and for

135 48 h at room temperature. The pH at time of equilibrium was determined using a pH meter,
136 and the samples were then filtered using 0.45 μm membrane filters. The supernatants were
137 analysed for Al, Ca, Fe, magnesium (Mg) and P using ICP-AES; and the leached
138 concentrations determined were used as background concentration for the precipitation test
139 before adding P.

140 Precipitation test was then conducted to determine at which pH, and Ca and P concentrations
141 the calcium phosphate precipitation might occur. The tests were performed in conditions
142 simulating the P adsorption experiments. Aliquots of 100 ml of deionized water were placed in
143 200 ml acid washed polyethylene bottles and then agitated with different concentration of Ca
144 and/or Fe (the concentration of Ca and/or Fe was determined based on the result of the
145 exchangeable test wherein some sludges leached Ca while some leached both Ca and Fe).
146 Thereafter, pH was adjusted using hydrochloric acid (0.01M) and potassium hydroxide (0.1M),
147 prior to adding the P stock solution. The mixtures were then agitated on a rotary shaker for
148 48h before being filtered using 0.45 μm membrane filter and then analysed for Ca, Fe and P.
149 Any reduction in the concentrations of Ca, Fe and P after the reaction time would indicate a
150 reaction taking place. To further probe the reaction taking place and the possible mechanism,
151 samples of the sludges before and after reaction with the P stock solution were examined using
152 Fourier transform infrared spectroscopy (FTIR); the spectrum was scanned from 500 to 4000
153 cm^{-1} .

154 **2.3.2 Linkage with inherent properties**

155 To identify which of the measured sludge properties gives the most explanation of variance in
156 P retention (uptake and maximum), a multiple linear regression analysis was conducted.
157 Pearson's correlation coefficients were computed to find out if there is high correlation between
158 the physicochemical properties of the dewatered sludges. Due to the high correlations found
159 between the measured physicochemical properties of the seventeen dewatered sludges,
160 rotated principal component analysis (PCA) was performed, using Varimax rotation method,
161 to reduce the number of predictor variables which are highly correlated (multicollinearity) from

162 eleven single variables to three uncorrelated linearly principal components. The produced
163 component scores were then used as predictors (independent variables) in addition to initial
164 pH of the solution in a multiple linear regression model. P uptakes at seven initial P
165 concentrations, P adsorption maxima and Freundlich constant were chosen as the outcome
166 (dependent) variables.

167 IBM SPSS statistic software (version 20) was used for statistical analyses. The Shapiro-Wilk's
168 test and data visualization by histograms, normal Q-Q plots and box plots were used to assess
169 the normal distribution of the experimental data. Where data was not normally distributed, a
170 transformation was performed for data to obtain a normal distribution.

171 **3. Results and discussion**

172 **3.1 General physicochemical characterization**

173 The dewatered waterworks sludges had highly variable physicochemical properties (see
174 Table 1). The main constituent of the sludges, by weight was either aluminium (0.39 – 15.2) %
175 or iron (0.59 – 29.8) %. It was evident that the Al and Fe contents of the sludges were
176 dependent on the primary coagulant used during the water treatment process. Ten of the
177 sludges were Fe-based, and the rest (including one sludge which contains both Al and Fe)
178 were Al-based. The total specific surface areas (TSSA) of the sludges ranged from 97 to 468
179 m²/g (see Table 1).

180 TC and organic carbon (OC) of the Al- and Fe-based sludges ranged from 53.7 to 177.4 and
181 53.1 to 177.4 mg/g, respectively as shown in Table 1. Also, it can be seen that there is
182 negligible difference between the TC and OC content of the sludges. This implies that the
183 content of most common inorganic carbon in the sludges; i.e. calcium carbonate and calcium
184 magnesium carbonate is minimal. TC has a negative impact on the P adsorption capacity of
185 dewatered sludges by retarding P diffusion into the micropores (Makris et al., 2005). However,
186 Yang et al. (2006) found that during the adsorption process, OC exchanges with P which
187 replaces it on the surface of the sludges, thus implying that more exchangeable OC can
188 enhance P retention by the sludges. In our study, it was not possible to isolate the effect of TC

189 and OC on P retention; however, results of the FTIR test shows that the carboxyl group bands
190 was changed after the sludges reacted with P, indicating the replacement of OC with the
191 phosphate ions on the surface of the sludge. The XRD diffraction patterns reveal sharp
192 diffraction characteristic (peaks) for GU, BS, HO, CA, AR, HU, SF and CF sludges; and these
193 were defined as: quartz for HO, HU and CF; graphite and iron molybdenum for GU; Lithium
194 phosphate and calcium manganese oxide for CA; cronosite and lavendulan for AR, graphite
195 for SF and mica and nimite-1 in addition to quartz for CF (see Table 1). Interestingly, the two
196 mineral peaks (mica and nimite-1) of CF which is a Fe-based sludge, contain iron and
197 aluminium ions. This indicates that the iron and aluminium metals alloys are in crystalline form.
198 This might impact on the adsorption behaviour of the CF sludge via reduction of the available
199 reactive surfaces for P retention. In addition, two crystalline peaks of graphite from carbon for
200 GU and SF which are both Al-based sludges, would suggest reduced cation and anion ions
201 leachability from these sludges, and this could restrict the adsorption process into aluminium
202 oxide especially for the SF sludge which has a high TC content.

203 Table 1 Physicochemical properties of the seventeen dewatered waterworks sludges

Properties		GU	BS	MO	HO	CA	WD	FO	HH	AR	OS	HU	WY	WA	BU	SF	CF	BG
Al	mg/g	112.81	4.59	3.89	65.35	6.80	104.22	21.16	5.16	5.87	105.34	151.88	4.84	108.78	5.80	122.29	50.05	7.71
Ca		1.16	6.83	2.65	1.90	3.33	1.80	3.17	3.06	24.87	0.88	3.21	0.89	0.93	1.47	0.63	12.56	6.67
Fe		17.00	298.10	257.80	143.29	255.46	9.75	241.69	193.85	277.72	28.73	8.25	287.34	5.94	212.09	13.91	245.79	257.99
P		0.24	0.61	0.39	0.65	0.29	0.70	0.43	0.44	0.35	0.60	4.78	0.77	0.68	0.61	0.47	3.19	1.70
Mg		0.66	0.47	0.20	1.38	0.43	0.44	0.25	0.81	0.28	0.79	0.97	0.23	0.57	0.31	0.20	9.15	0.47
Mn		0.33	0.94	0.79	0.57	0.45	0.29	2.32	0.37	0.52	0.40	0.66	1.28	0.43	0.17	0.42	1.55	1.27
Zn		1.02	0.19	0.40	1.71	0.09	0.47	0.09	1.85	0.08	1.71	0.12	0.16	1.22	1.74	0.84	0.28	0.50
Al_{oxa}		110.12	1.14	1.85	58.63	1.02	95.28	17.36	1.36	2.99	88.26	105.51	3.46	96.02	4.67	75.68	2.62	4.14
Fe_{oxa}		13.35	143.08	149.52	72.41	144.48	3.68	121.33	121.38	113.63	14.42	2.52	146.37	4.64	138.48	6.96	118.09	101.10
p_{oxa}		0.22	0.23	0.24	0.34	0.28	0.28	0.23	0.30	0.21	0.27	0.69	0.34	0.30	0.25	0.28	0.24	0.52
Cl⁻		0.11	0.22	0.16	0.16	0.21	0.24	0.30	0.33	0.59	0.11	0.22	0.27	0.14	0.22	0.56	0.76	0.48
SO₄		0.81	4.06	6.93	3.86	7.45	1.88	4.26	4.51	6.32	1.19	2.72	8.55	0.33	2.81	0.26	0.71	0.22
TC		119.6	110.8	117.4	105.2	115.9	119.6	137.	161.9	88.62	170.6	75.21	113.7	154.4	154	177.4	53.7	144.4
OC		118.9	110.8	117.4	105.2	115.9	119.1	137	161.9	88.62	170.1	74.2	113.7	154	153.6	177.4	53.1	144.4
TSSA	m ² /g	364.1	203.4	186.4	414.5	219.8	468	120.3	131.9	97.02	206.9	390.4	132.3	210.1	157.2	181.8	296.3	125.2
EC	μs/cm	455.5	522.8	488.3	665.7	410.7	723.1	378	375.8	1239.3	421.3	541.5	843.4	688	828	329.2	1073.1	471.1
PH	---	6.26	5.47	4.48	5.49	4.09	6.27	5.49	4.55	6.64	6.05	7.06	4.3	6.31	4.75	6.13	6.99	5.89
Crystalline minerals		Graphite, Iron Molybdenum	Lithium boride	---	Quartz	Lithium phosphate, Calcium manganese oxide	---	---	---	Cronusite, Lavendulen	---	Quartz	---	---	---	Graphite	Quartz, Mica, Nimit-1	---

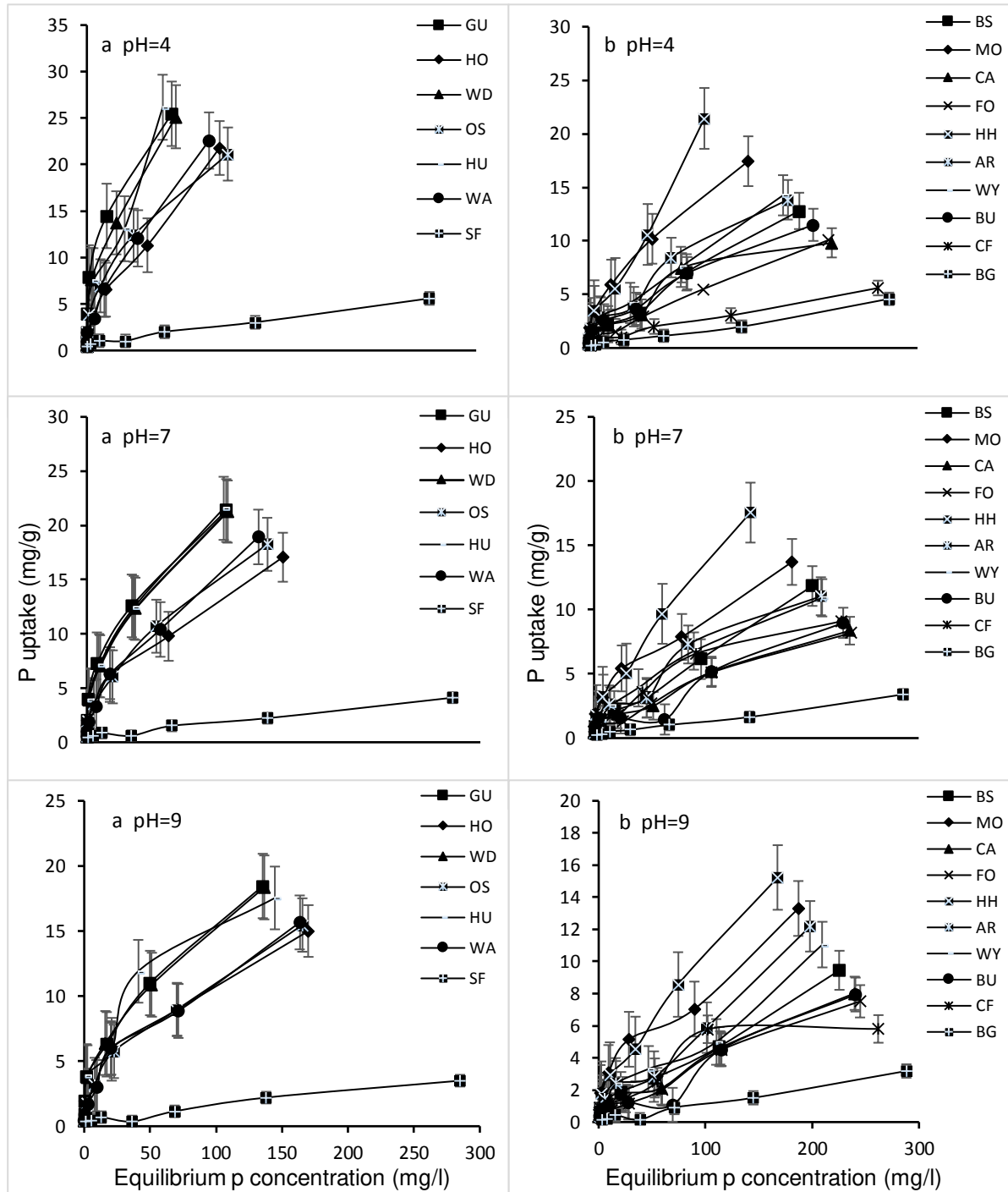
205 In general, XRD patterns for the sludges showed apparent poorly ordered particle distribution
206 of Al and Fe minerals within the Al- and Fe-based sludges (with the exception of CF); this
207 implies that the Al and Fe sludges are in the amorphous phases. Amorphous oxide phases are
208 assumed to be extracted with acidified ammonium oxalate and associated with non-crystalline
209 phase of metal oxides. Thus, the quantity of Al_{oxa} and Fe_{oxa} in the sludges were determined
210 using this method. Results show that the amorphous Al and Fe oxides represent 61.9 to 97.6%
211 of total Al for the Al-based sludges and 39.2 to 65.3% of total Fe for the Fe-based sludges (see
212 table 1). P uptake is strongly linked to amorphous Al and Fe concentrations and the variation
213 in oxalate extractable Al and Fe has been shown to account for differences in P retention by
214 dewatered waterworks sludges (Dayton and Basta, 2005; Elliott et al., 2002).

215 **3.2 Adsorption isotherm study**

216 Figure 1 shows the isotherm of P uptake by the sludges. For ease of comparison, the Al- and
217 Fe-based sludges were grouped separately. To determine if there was any significant
218 difference in P uptake between the sludges; a one-way ANOVA was used. The results revealed
219 significant differences in P uptake between the sludges ($p= 0.002$). These findings are
220 consistent with those of Makris et al. (2005) who studied the P sorption/desorption
221 characteristics and kinetics for seven dewatered waterworks sludges and found that the Al-
222 based sludges had higher adsorption capacity than the Fe-based sludges.

223

224



225

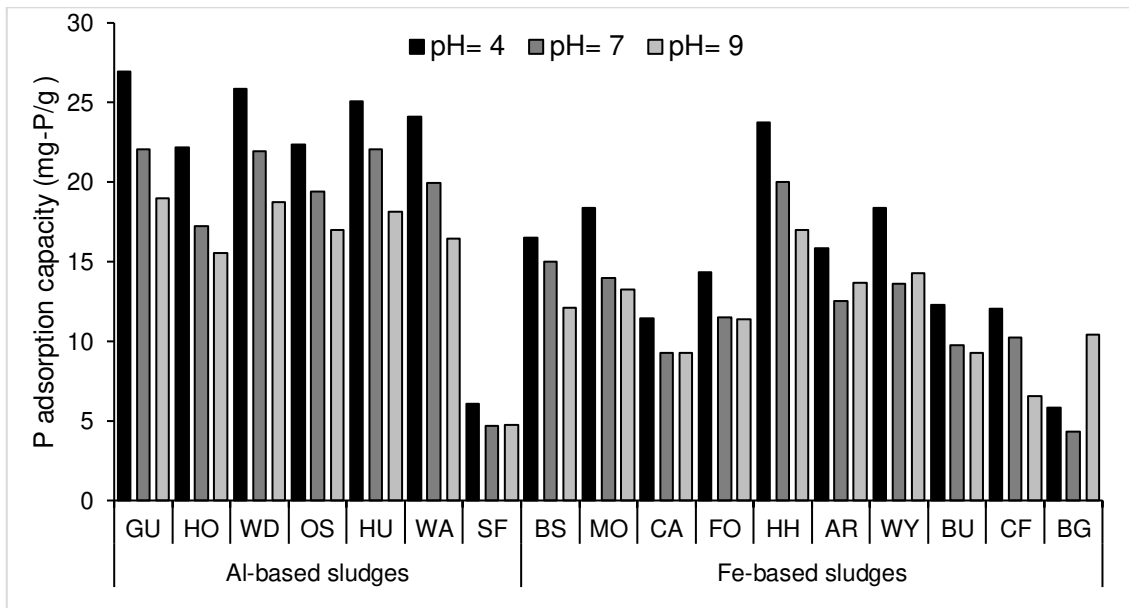
226 Figure 1 Isotherms of P uptake by the seventeen dewatered water sludges (at initial pHs of 4,
 227 7 and 9; t=48 hours; plots to the left and right refer to, respectively, aluminium- and iron-based
 228 sludges).

229 Further data analysis show that the P adsorption data was well fitted with the Freundlich model;
 230 and that the adsorption density value for all the sludges was > 1 and ranged from 1.40 to 2.79.

231 For most sludges, the bonding energy related constant decreased as the adsorption density

232 increased, in accordance with preferential adsorption occupying surface sites in order from
233 strongest to weakest binding strength (Apak, 2013).

234 P adsorption capacities obtained from the fitting of the Langmuir model (see figure 2) shows
235 generally that sludges had variable adsorption capacities which increased with decrease initial
236 pH solution. This suggests that P adsorption by the sludges is favourable at acidic conditions.
237 It should be noted that the adsorption capacities reported herein relate to the equilibrium
238 concentration of P in solution. Therefore, using the adsorbents at very low P concentration
239 means the process would be operating under the most unfavourable condition. To compare
240 the P adsorption capacity (as determined by the Langmuir model for those sludges with good
241 fitting); one-way ANOVA analysis was used. The results of the test showed that there was
242 significant difference in adsorption capacities between the Al- and Fe-based sludges ($P <$
243 0.001). This is in agreement with Makris et al. (2005) which showed higher P adsorption
244 capacity for Al-based sludge than Fe-based sludges. Elliott et al. (2002) also reported similar
245 findings in P adsorption between Al- and Fe-based sludges. In addition, the adsorption capacity
246 is related with SSA which in turn depends on the metal oxide. Makris et al. (2004) found that
247 Al-based sludges have higher SSA than Fe-based sludges, resulting in the differences in their
248 adsorption capacities. In our study, higher TSSA and P adsorption capacity were found for Al-
249 based sludges with the exception of SF sludge. The SF sludge has the highest carbon content
250 (crystalline – graphite) which restricts the contact surfaces available for P retention.



251

252 Figure 2 P adsorption capacities of Al- and Fe-based sludges calculated from fitting Langmuir
 253 model at three initial pH solution values.

254 **3.3 P retention – Mechanisms**

255 Table 2 presents results of the exchangeable ions test. Results show that the cations
 256 concentrations decreased as the initial solution pH increased. The pH at equilibrium was either
 257 increased or decreased relative to the initial pH. This could be explained by the fact that during
 258 the agitation, the hydroxyl groups on the surface of the sludge and also cations and anions (as
 259 Ca, Mg, Cl⁻, SO₄²⁻, TOC) released into the solution influence the increase or decrease of the
 260 pH from its initial value. The P released from the sludges was low across the three initial pHs.
 261 This P originates from the raw water and becomes part of the structure of the dewatered
 262 sludges; and it is minimally released over time (Makris, 2004). The concentration of Ca
 263 released across the three initial pHs was generally higher than that observed for the other
 264 cations and ranged from 3.0 mg/l to 34.5 mg/l at initial pH 4. The amount of exchangeable Ca
 265 was proportional with Ca content of the sludges with the exception of GU and SF, both of which
 266 contain carbon as graphite (crystalline), resulting in low exchangeable ions. In addition,
 267 significant Fe concentrations were observed for BS, CA, HH and WY sludges with 1.38; 3.73;
 268 2.36 and 1.54 mg/l of Fe respectively at initial pH 4. The pHs were acidic for most of the sludges
 269 except for AR, HU and CF which all had approximately neutral equilibrium pH. The neutral pH

270 of the three sludges resulted from the combination of the initial pH and pH at equilibrium,
271 combined with increased Ca concentration which might then encourage calcium phosphate
272 precipitation (Del Bubba et al., 2003).

273 Table 2 Equilibrium pH and the released concentrations of aluminium, iron, calcium, magnesium and phosphorus after agitating one gram of each
 274 sludge in 100 ml of deionized water with three initial pH values for 48 h (n=2)

sludge	pH* 4						pH* 7						pH* 9					
	pH**	Al mg/l	Ca mg/l	Fe mg/l	Mg mg/l	P mg/l	PH**	Al mg/l	Ca mg/l	Fe mg/l	Mg mg/l	P mg/l	PH**	Al mg/l	Ca mg/l	Fe mg/l	Mg mg/l	P mg/l
GU	5.93	0.027	4.345	0.003	0.447	0.549	6.07	0.018	3.228	0.001	0.428	0.441	6.08	0.016	2.939	0.001	0.411	0.402
BS	5.15	0.024	13.17	1.381	1.251	0.413	5.23	0.038	11.95	1.31	1.179	0.407	5.25	0.028	11.3	1.167	1.127	0.381
MO	4.28	0.346	6.679	0.909	0.709	0.384	4.35	0.259	6.141	0.892	0.701	0.378	4.38	0.235	6.072	0.889	0.714	0.373
HO	5.36	0.121	11.94	0.146	0.928	0.391	5.49	0.095	11.21	0.095	0.875	0.375	5.47	0.075	10.11	0.064	0.888	0.357
CA	4.25	0.554	12.28	3.734	1.068	0.355	4.28	0.442	11.58	3.526	1.035	0.354	4.29	0.43	11.73	3.567	1.03	0.334
WD	5.76	0.045	7.778	0.0012	0.919	0.377	5.98	0.015	6.929	0.0011	0.92	0.353	6.11	0.017	7.299	0.001	0.911	0.352
FO	5.35	0.032	8.923	0.035	0.724	0.402	5.52	0.031	7.541	0.068	0.72	0.395	5.53	0.029	6.494	0.086	0.593	0.379
HH	4.93	0.319	4.596	2.363	0.594	0.382	5.05	0.222	3.138	2.161	0.425	0.376	5.06	0.291	3.707	2.619	0.488	0.366
AR	7.33	0.033	34.50	1.081	0.524	0.388	7.41	0.021	33.88	0.959	0.504	0.379	7.42	0.007	33.21	0.612	0.5	0.375
OS	5.37	0.072	3.955	0.009	0.704	0.38	5.74	0.028	2.709	0.008	0.601	0.371	5.75	0.027	2.822	0.0075	0.597	0.326
HU	7.08	0.011	12.06	0.001	0.944	0.4	7.10	0.01	11.43	0.001	0.981	0.398	7.15	0.01	10.9	0.001	0.981	0.392
WY	3.85	0.669	6.495	1.541	0.581	0.392	3.96	0.657	6.028	1.497	0.561	0.342	3.96	0.542	5.823	1.357	0.521	0.334
WA	4.75	1.58	5.257	0.006	0.489	0.346	4.81	0.932	5.049	0.005	0.497	0.344	4.81	0.916	4.736	0.003	0.463	0.299
BU	4.15	0.635	5.841	0.400	0.718	0.351	4.25	0.425	5.459	0.33	0.706	0.347	4.29	0.349	5.444	0.303	0.699	0.312
SF	4.87	0.051	2.964	0.003	0.938	0.621	5.89	0.042	2.404	0.002	0.227	0.548	5.99	0.04	2.213	0.001	0.215	0.401
CF	7.46	0.045	13.64	0.195	0.938	0.396	7.58	0.032	10.14	0.065	0.761	0.395	7.59	0.026	9.388	0.051	0.692	0.371
BG	6.50	0.04	3.431	0.098	0.423	0.378	6.64	0.032	2.361	0.094	0.332	0.378	6.66	0.029	2.325	0.047	0.327	0.356

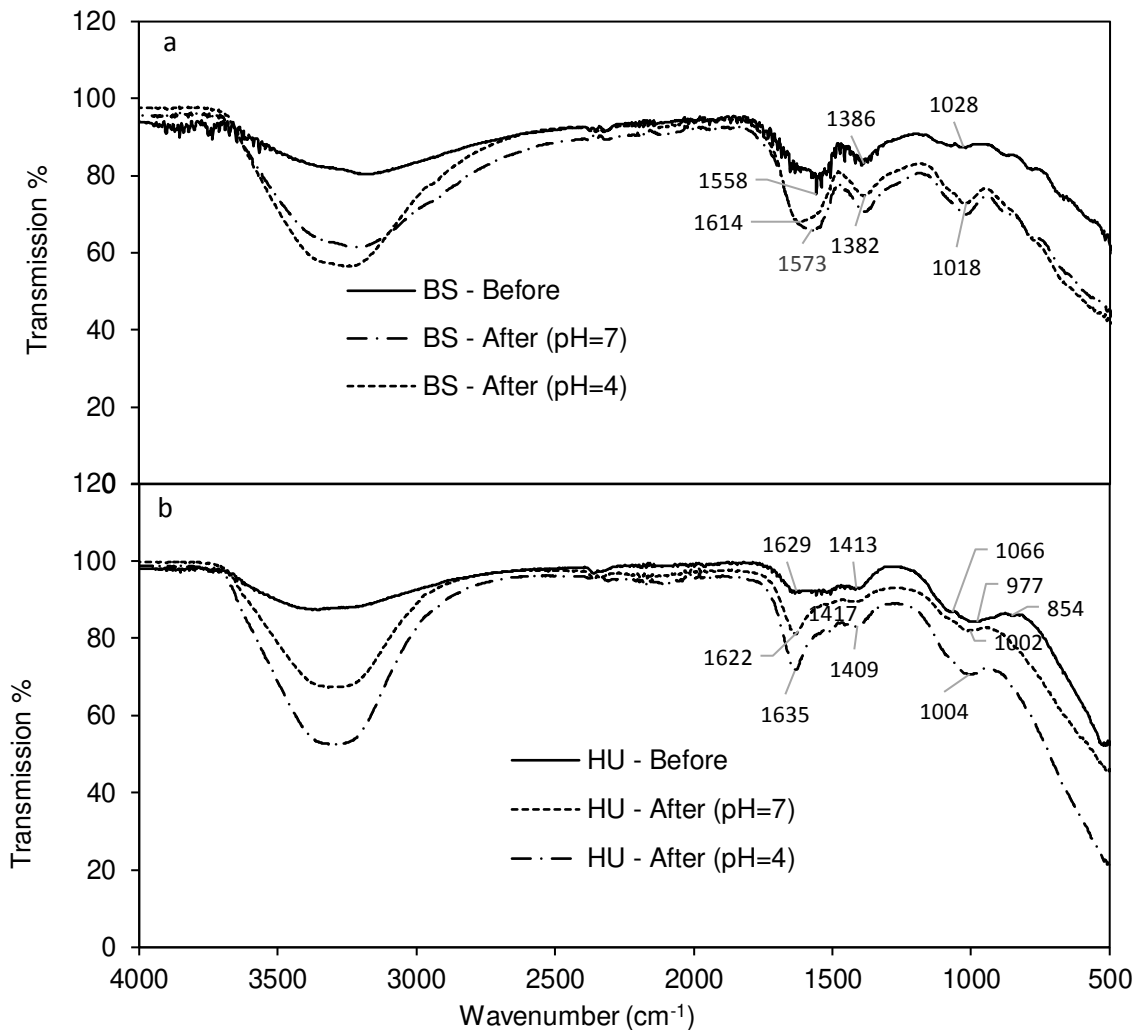
* initial pH solution, ** pH at equilibrium time (after 48 hrs agitation)

276 Furthermore, precipitation test was conducted to determine the conditions of pH, Ca, Fe and
277 P concentrations which might cause phosphate precipitation. To decide which equilibrium pH,
278 and Ca and Fe concentrations across the three initial pHs should be used in the precipitation
279 test; a one-way ANOVA analysis was performed to find out if there is any significant differences
280 in these values across the initial pHs. The results showed that there was no significant
281 differences in the variation of the pH at equilibrium and the Ca and Fe concentrations ($p > 0.05$).
282 Thus, different samples with different pH values and Ca and Fe concentrations were used
283 depending on the exchangeable ions test; while the P concentration values used were based
284 on the change in P uptake over the range of initial P concentrations. Results obtained (not
285 shown) indicate that no significant changes between initial and final concentration of both Ca
286 and P to precipitate calcium phosphate minerals occurred at pH less than 7.3. Whereas at pH
287 > 7.3 , preliminary phosphate retention via precipitation mechanism was found at high initial P
288 concentrations. Based on the molar ratio of Ca to P (0.5), it can be proposed that monocalcium
289 phosphate was the precipitated metal. The formation of monocalcium phosphate metal is
290 dependent on the availability of phosphoric acid (H_3PO_4), which is one of the orthophosphate
291 species; in addition to calcium at alkaline condition. The amount of H_3PO_4 is minimal at neutral
292 to alkaline pH solution, thus the calcium phosphate precipitation in this study can be considered
293 to be minimal. The P precipitation retention mechanism as calcium phosphate minerals will
294 spontaneously occur and is the dominant mechanism at pH > 8 (Khelifi et al., 2002; Søvik and
295 Kløve, 2005). In this study, high equilibrium pH (> 7.3) was observed for AR and CF sludges,
296 both of which also have the highest Ca content (table 1) and exchangeable Ca (table 2). In
297 these conditions, P retention by calcium phosphate precipitation is minimal and P adsorption
298 by Al and Fe oxides are the main possible mechanisms for the AR and CF sludges.

299 For samples that contained Fe ions, prior to reaction with the phosphate ions; the initial Fe
300 precipitated as iron oxides when the dissolved Fe had reacted with sodium hydroxide ions
301 which had been added for pH adjustment. Thus the final Fe concentrations were minimal and
302 below the limit of detection. After adding the P stock solution, the iron precipitates have the

303 ability to adsorb phosphate ions via surface complexation mechanism through the formation of
304 inner sphere and/or outer sphere complexes with the iron precipitates.

305 The P retention mechanism was further investigated by analysing the FTIR spectra of the
306 sludges before and after reaction with the phosphate ions (see figure 3). Results reveal that
307 without phosphate adsorption, the FTIR spectra of the sludges had a strong hydroxyl stretching
308 (e.g. 3200 cm^{-1} for BS and HU) and bending (1558 cm^{-1} for BS and HU) vibrations, which are
309 due to physically adsorbed water molecules; while the band at 1413 and 1386 cm^{-1} could be
310 assigned to stretching vibration of C-O and deformation vibration of C-H for carboxyl functional
311 groups (Izquierdo et al., 2012). Additionally, deformation vibrations of multi-centred hydroxyl
312 groups of iron and aluminium oxides (Fe-OH, Al-OH) of the sludges were observed at 1028
313 cm^{-1} bands for the Fe-based sludge and two bands of 1066 and 977 cm^{-1} for the Al-based
314 sludges (Zhang et al., 2007). After reaction with phosphate ions, the FTIR spectrums of the
315 sludges showed clear changes. The peaks of physically adsorbed water and stretching and
316 deformation of carboxyl groups became broad and intensive which is attributed to replacement
317 of H_2O , C-O and C-H during the phosphate adsorption. Moreover, the peaks of bending
318 vibration of multi-centred hydroxyl groups for Fe-OH and Al-OH completely disappeared, while
319 a new broad and intensive peak appeared at 1018 and 1004 cm^{-1} for Fe and Al oxides
320 respectively. This peak could be attributed to the formation of inner sphere surface
321 complexation between phosphate ions and oxides (Persson et al., 1996); and outer sphere
322 surface by exchanging phosphate ions with hydroxyl group on the surface of dewatered sludge.
323 The FTIR results indicate that the surface complexation of inner and outer sphere played a key
324 role in the adsorption mechanism.



325

326 Figure 3 FTIR spectra of (a) Fe-based sludge and (b) Al-based sludge; before and after
 327 adsorption test with 10 mg/l initial P concentration at pH 4 and 7.

328 **3.4 P retention –Linkage with inherent properties**

329 The results of the principal component analysis are presented in Table 3. The properties which
 330 combine in the same principal component (PC) could be identified as; PC1- metal content and
 331 TSSA - related component (high loadings for Al, Fe, Al_{oxa}, Fe_{oxa} and TSSA, total variance =
 332 42.75%); PC2- Ca content, exchangeable Ca (Ca_{ex}), TC, total organic carbon (TOC) related
 333 component (total variance = 34.56%); and PC3 - SO₄²⁻ content and sludge pH related
 334 component (total variance = 16.48%). Combined, the three PCs could explain 93.8% of the
 335 total variance in the physicochemical characteristics. The scores of the three PCs and initial
 336 pH of the incubation solution were then used as predictors in multiple regression analysis,
 337 where the outcome variable was the amount of P removed at different initial P concentrations.

338 The largest and most significant explanation in variability of P removal was found at initial P
339 concentration of 80 mg/l. When PC1 was entered first, it accounted for 52.9% of variance in P-
340 uptake ($p < 0.001$). When PC2 was entered next into the model, an additional 4.5% significant
341 P removal was recorded ($p < 0.05$); and when PC3 and the initial pH of incubation solution
342 were entered, a 2.9% and 4.4% explanation, respectively of significant variability in P-uptake
343 ($p < 0.05$) was obtained. Thus the total significant variance in P-uptake in the linear regression
344 model that could be explained by these characteristics of the sludges and initial pH solution
345 was 64.6% ($p < 0.001$). In the case of 160 mg/l and 320mg/l initial P concentrations, the multiple
346 linear regression analysis exhibited similar pattern, but the total explainable variance in P-
347 uptake became less by excluding the effect of sulphate content and pH related component
348 (PC3). By following the same procedure for the lower initial P concentration, the total
349 explainable variance in P-uptakes by the three predictors (initial pH solution was excluded)
350 increased with increasing initial P concentration except for the P-uptake at 5 mg/l initial P
351 concentration. At 5 mg/l, PC3 and initial pH solution were not significantly linked to the P-
352 uptake and the metal content related factor; and the Ca, Ca_{ex} , TC and TOC related factor
353 combined together, explained 55.9% in the variance in P-uptake. The metal content related
354 component (PC1) was the most significant predictor in explaining the variance in P-uptakes
355 across the initial P concentration.

356 The same procedure above was used to determine the physicochemical characteristics of the
357 sludges which had the most effect on the maximum P adsorption capacity as calculated by the
358 Langmuir model. The scores of the three PCs and the initial solution pH were used as
359 predictors in multiple linear regression analysis, where the calculated P adsorption capacity
360 was used as the outcome variable. Combined together, PC1 and initial solution pH accounted
361 for 44.8% significant variability of calculated P adsorption maxima, while PC2 and PC3 were
362 not significantly correlated with the P adsorption maxima. As discussed previously, the best fit
363 for adsorption data for all the sludges at the three pHs was given by Freundlich model.
364 Therefore, to identify which of the physicochemical properties of the sludges had the most
365 effect on the Freundlich bonding energy related parameter (K_f), the same procedure above

366 was used. The significant variances in P-uptakes and adsorption parameters explained by the
367 physicochemical properties of the sludges and initial pH solution are presented in the Table 3.
368 The metal content and TSSA related component (PC1); Ca content, exchangeable Ca, TC and
369 OC related component (PC2), and initial solution pH were significantly related to K_f Freundlich
370 parameter. A total 78.4% of variability in K_f ($p < 0.001$) was explained by these predictors at
371 significant levels < 0.001 , < 0.01 , and < 0.01 respectively.

372

373

374

375

376

377

378

379

380

381

382

383

384 Table 3 Principal component analysis of the physicochemical characteristics of the seventeen dewatered waterworks sludges; and linear
 385 regression analysis between the three principal components scores and initial pH solution as predictors, and amount of P-uptake at different initial
 386 P concentration, P adsorption capacity maxima and Freundlich P bonding energy related constant as outcomes variables.

Principal component	PC1	PC2	PC3	Independent variable	PC1	PC2	PC3	pH	TV%
Eigenvalue	5.626	3.668	1.023		Percentage of explainable variance				
Proportion of variance (%)	42.745	34.563	16.477	q ₁ ^a	45.3 ^{***}	6.1 [*]	NOT Sig.	NOT Sig.	55.9 ^{***}
Cumulative proportion of variance (%)	72.745	77.308	93.785	q ₂ ^a	28.9 ^{***}	9.3 ^{**}	NOT Sig.	NOT Sig.	38.2 ^{***}
	Rotated factor loading			q ₃ ^a	30.8 ^{***}	10.1 ^{**}	6.1 [*]	NOT Sig.	46.9 ^{***}
Variable	PC1	PC2	PC3	q ₄ ^a	36.9 ^{***}	8.1 ^{**}	8.2 ^{**}	NOT Sig.	53.2 ^{***}
Al	0.925	-0.044	0.33	q ₅ ^a	52.9 ^{***}	4.5 [*]	2.9 [*]	4.4 [*]	64.6 ^{***}
Fe	-0.918	0.255	-0.256	q ₆ ^a	46.4 ^{***}	6.5 ^{**}	NOT Sig.	6.9 [*]	59.8 ^{***}
Al _{oxa}	0.953	-0.083	0.259	q ₇ ^a	42.3 ^{***}	4 [*]	NOT Sig.	9.5 ^{**}	55.8 ^{***}
Fe _{oxa}	-0.881	0.168	-0.402	Q _o ^b	34.4 ^{***}	NOT Sig.	NOT Sig.	10.4 [*]	44.8 ^{***}
Ca	-0.596	0.691	0.337	K _f ^c	66.4 ^{***}	6.2 ^{**}	NOT Sig.	5.8 ^{**}	78.4 ^{***}
Ca _{ex}	-0.154	0.915	-0.081	* explainable variance is significant at the 0.05 level					
SO ₄ ²⁻	-0.419	0.271	-0.801	** explainable variance is significant at the 0.01 level					
TC	0.019	-0.969	0.012	*** explainable variance is significant at the 0.001 level					
TOC	0.013	-0.969	0.009	^a P-uptakes ranged q ₁ , q ₂ , q ₃ , q ₄ , q ₅ , q ₆ , and q ₇ at initial P concentrations ranged 5, 10, 20, 40, 80, 160 and 320 mg/l; ^b calculated P adsorption maxima determined from fitting the linearized Langmuir model; ^c bonding energy related constant calculated from fitting the linearized Freundlich model; For the principal component table, variable with high component loading are shown in bold					
TSA	0.756	0.563	0.027						
pH	0.438	0.343	0.805						

388 **4. Conclusion**

389 This study aimed at contributing to practical reduction of eutrophication caused by excess
390 phosphorus (P) loading to the environment. Specifically, it was focused on advancing our
391 fundamental understanding of P reduction by novel industrial by-products, using dewatered
392 drinking water treatment sludge as P adsorbent. Findings have shown that aluminium (Al) and
393 iron (Fe) based dewatered waterworks sludges have considerable variability in their
394 physicochemical properties; and the difference in their P retention behaviour can be explained
395 by the amount of reactive Al and Fe available, the total specific surface area, and in some
396 cases, the presence of crystalline phases of total carbon and other minerals. Al-based sludges
397 tended to have higher total specific surface areas and thus, higher adsorption capacity. P
398 retention was shown to be generally through surface complexation, ligand exchange and/or
399 precipitation. In particular, FTIR results indicate that surface complexation of inner and outer
400 sphere played a key role in the adsorption mechanism. In almost all cases, adsorption data
401 was well described by the Freundlich model indicating the heterogeneity of P adsorption on
402 the surface of the sludges. However, adsorption data for two of the sludges which were Al
403 based were best fitted with the Langmuir model, with minimal leaching of Al, Calcium and
404 sulphate ions observed. This implies that P adsorption by surface complexation is the only
405 possible mechanism for the two sludges.

406 **Acknowledgements**

407 Authors gratefully acknowledge the support of the technical staff at the Cardiff University
408 School of Engineering, in particular Mr. Jeff Rowlands. The first author would like to thank the
409 Iraqi Ministry of Higher Education and Scientific Research for financial support.

410 **References**

- 411 Apak, R., 2013. Adsorption of heavy metal ions on soil surfaces and similar substances:
412 theoretical aspects. *ChemInform* 44.
- 413 Babatunde, a O., Zhao, Y.Q., Burke, a M., Morris, M. a, Hanrahan, J.P., 2009.
414 Characterization of aluminium-based water treatment residual for potential phosphorus
415 removal in engineered wetlands. *Environ. Pollut.* 157, 2830–6.

- 416 doi:10.1016/j.envpol.2009.04.016
- 417 British Standards Institution, 1990. Methods of test for soils for civil engineering purposes
418 (BS 1377). Part 2 Classif. tests.
- 419 Cerato, A.B., Lutenegeger, A.J., 2002. Determination of surface area of fine-grained soils by
420 the ethylene glycol monoethyl ether (EGME) method. *Geotech. Test. J.* 25, 315–321.
421 doi:10.1520/GTJ11087J
- 422 Dayton, E. a, Basta, N.T., 2005. A Method for Determining the Phosphorus Sorption Capacity
423 and Amorphous Aluminum of Aluminum-Based Drinking Water Treatment Residuals. *J.*
424 *Environ. Qual.* 34, 1112. doi:10.2134/jeq2004.0230
- 425 Del Bubba, M., Arias, C. a, Brix, H., 2003. Phosphorus adsorption maximum of sands for use
426 as media in subsurface flow constructed reed beds as measured by the Langmuir
427 isotherm. *Water Res.* 37, 3390–400. doi:10.1016/S0043-1354(03)00231-8
- 428 Elliott, H. a, O'Connor, G. a, Lu, P., Brinton, S., 2002. Influence of water treatment residuals
429 on phosphorus solubility and leaching. *J. Environ. Qual.* 31, 1362–1369.
430 doi:10.2134/jeq2002.1362
- 431 Goldberg, S., Johnston, C.T., 2001. Mechanisms of Arsenic Adsorption on Amorphous
432 Oxides Evaluated Using Macroscopic Measurements, Vibrational Spectroscopy, and
433 Surface Complexation Modeling. *J. Colloid Interface Sci.* 234, 204–216.
434 doi:10.1006/jcis.2000.7295
- 435 Ippolito, J. a, Barbarick, K. a, Elliott, H. a, 2011. Drinking water treatment residuals: a review
436 of recent uses. *J. Environ. Qual.* 40, 1–12. doi:10.2134/jeq2010.0242
- 437 Izquierdo, M., Marzal, P., Gabaldón, C., Silvetti, M., Castaldi, P., 2012. Study of the
438 Interaction Mechanism in the Biosorption of Copper(II) Ions onto *Posidonia oceanica*
439 and Peat. *CLEAN - Soil, Air, Water* 40, 428–437. doi:10.1002/clen.201100303
- 440 Johansson, L., Gustafsson, J.P., 2000. Phosphate removal using blast furnace slags and
441 opoka-mechanisms. *Water Res.* 34, 259–265. doi:10.1016/S0043-1354(99)00135-9
- 442 Khelifi, O., Kozuki, Y., Murakami, H., Kurata, K., Nishioka, M., 2002. Nutrients adsorption
443 from seawater by new porous carrier made from zeolitized fly ash and slag. *Mar. Pollut.*
444 *Bull.* 45, 311–315. doi:10.1016/S0025-326X(02)00107-8
- 445 Makris, K.C., 2004. Long-Term Stability of Sorbed Phosphorus By Drinking-Water Treatment
446 Residuals: Mechanisms and Implications 198p.
- 447 Makris, K.C., El-Shall, H., Harris, W.G., O'Connor, G. a., Obreza, T. a., 2004. Intraparticle
448 phosphorus diffusion in a drinking water treatment residual at room temperature. *J.*
449 *Colloid Interface Sci.* 277, 417–423. doi:10.1016/j.jcis.2004.05.001
- 450 Makris, K.C., Harris, W.G., O'Connor, G. a., Obreza, T. a., Elliott, H. a., 2005.
451 Physicochemical properties related to long-term phosphorus retention by drinking-water
452 treatment residuals. *Environ. Sci. Technol.* 39, 4280–4289. doi:10.1021/es0480769
- 453 McKeague, J. a., Day, J.H., 1966. DITHIONITE- AND OXALATE-EXTRACTABLE Fe AND Al
454 AS AIDS IN DIFFERENTIATING VARIOUS CLASSES OF SOILS. *Can. J. Soil Sci.* 46,
455 13–22. doi:10.4141/cjss66-003
- 456 Persson, P., Persson, P., Nilsson, N., Nilsson, N., Sjöberg, S., Sjöberg, S., 1996. Structure

- 457 and Bonding of Orthophosphate Ions at the Iron Oxide-Aqueous Interface. *J. Colloid*
458 *Interface Sci.* 177, 263–275. doi:10.1006/jcis.1996.0030
- 459 Søvik, a. K., Kløve, B., 2005. Phosphorus retention processes in shell sand filter systems
460 treating municipal wastewater. *Ecol. Eng.* 25, 168–182.
461 doi:10.1016/j.ecoleng.2005.04.007
- 462 Yang, Y., Zhao, Y., Babatunde, a, Wang, L., Ren, Y., Han, Y., 2006. Characteristics and
463 mechanisms of phosphate adsorption on dewatered alum sludge. *Sep. Purif. Technol.*
464 51, 193–200. doi:10.1016/j.seppur.2006.01.013
- 465 Zhang, G.-S., Qu, J.-H., Liu, H.-J., Liu, R.-P., Li, G.-T., 2007. Removal Mechanism of As(III)
466 by a Novel Fe–Mn Binary Oxide Adsorbent: Oxidation and Sorption. *Environ. Sci.*
467 *Technol.* 41, 4613–4619. doi:10.1021/es063010u
- 468